ELSEVIER

Chemical Engineering Journal 84 (2001) 223–237

Chemical Engineering Journal

www.elsevier.com/locate/cej

Laminar convection of non-Newtonian fluids in the thermal entrance region of coiled circular tubes

K.D.P. Nigam*, Shobha Agarwal, V.K. Srivastava

Chemical Engineering Department, Indian Institute of Technology, Hauz Khas, New Delhi-110 016, India

Received 15 September 1999; accepted 3 October 2000

Abstract

The governing equations for fully developed laminar flow and heat transfer in the thermal entrance region of circular curved tubes are solved numerically for power law fluids. Detailed descriptions of the secondary velocity profiles and temperature profiles as a function of Dean number, Prandtl number and power law index are provided to elucidate the significant role of secondary convection. Results for friction factors, asymptotic Nusselt numbers and Nusselt numbers in the thermal entrance region are computed and compared with the published experimental and theoretical results for Newtonian and power law fluids. Satisfactory agreement is found. For a given Prandtl and Dean number the Nusselt number increases with increases in power law index and the thermal entrance length is found to be shortened for dilatant fluids in comparison with the pseudoplastic fluids.

Keywords: Power law fluid; Coiled tube; Secondary flow; Entrance region; Heat transfer

1. Introduction

Hellically coiled, circular tubes have received attention in the literature due to their frequent use in heat exchangers, chemical reactors, chromatographic columns and other devices. They offer more efficient heat transfer, reduced back mixing and smaller space requirements compared with straight tubes. The enhancement of heat transfer and mass transfer in coils occurs due to the existence of a secondary flow which appears as twin, counter-rotating vortices in the cross-sectional plane. Dean [6,7] showed that a single dynamic similarity parameter, the Dean number ($N_{De} = N_{Re}\sqrt{a/b}$), where N_{Re} is Reynolds number and a and b are the radius of the tube and curvature, respectively can characterise the flow phenomena of Newtonian fluids in a coiled tube.

Comprehensive reviews of the flow of Newtonian fluids in curved pipes were published by Berger et al. [4], Ito [15], Tarbell and Samuels [36] and Nandakumar and Masliyah [23]. Most of the studies were confined to Newtonian fluids and very little attention has been paid to the flow of non-Newtonian fluids in curved circular tubes despite their importance in polymer, biomedical and biochemical processing. A comprehensive search of the literature on the flow of power law fluids in curved circular tubes has been listed in Table 1 and Table 2 for theoretical and experimental studies, respectively. Most of the theoretical analyses have limitations that prevent their use for design calculations.

A review of laminar heat transfer for Newtonian fluids in curved tubes has been published by Shah and Joshi [31]. Theoretical studies of power law fluids in coiled tubes include only those by Raju and Rathna [29], Hsu and Patankar [13] and Kewase and Young [17]. Experimental correlations have been reported by Rajasekharan et al. [28], Gupta and Mishra [11] and Nandapurkar and Raja Rao [39]. These are of little value in predicting the physics of heat transfer to power law fluids in curved, circular tubes because of their non-clarity of wall conditions and limitations of experimental parameters. Raju and Rathna's analysis [29] is unable to predict the effect of curvature on momentum and heat transfer for power law fluids in coiled tubes. Kewase and Young [17] developed a simple model for momentum and heat transfer of power law fluids in circular curved tubes using the momentum integral method, their satisfactory predictions of friction factor and asymptotic Nusselt number were computed only for the high values of Dean numbers ($N_{De} >$ 100). Hsu and Patankar [13] have numerically computed the fully developed Nusselt numbers of power law fluids in circular curved tube for the condition of constant wall heat flux. They reported that dilatant fluids exhibit higher Nusselt numbers than Newtonian fluids. Conversely, pseudoplastic fluids exhibit lower Nusselt numbers than Newtonian fluids.

Since Graetz [9], considerable literature has been published to understand the phenomenon of heat transfer to

* Corresponding author.

1385-8947/01/$ – see front matter
PII: S1385-8947(00)00376-4

Nomenclature

a	radius of the tube
A	defined in Eq. (5E)
b	radius of the curvature of the tube
B	defined in Eq. (5E)
c_p	specific capacity
d	diameter of the tube
f_c	friction coefficient in curved tube
f_s	friction coefficient in straight tube
f_w	defined in Eq. (5D)
K'_c	defined by Mujawar and Raja Rao in terms of n and μ_p
K_c	theal conductivity
L	length of the tube (or heated length of the tube)
m	$(n+1)/n$
M	defined by Mujawar and Raja Rao in terms of n and μ_p
n	power law index
n'_c	defined by Mujawar and Raja Rao in terms of n and μ_p
p	nondimensional pressure
P	dimensional pressure
r	nondimensional radial co-ordinate
R	dimensional radial co-ordinate
T	dimensionless temperature
T^*	dimensional temperature
T_b	bulk temperature
T^o	reference temperature
T_w	wall temperature
u, v, w	nondimensional velocities in r, θ, ϕ
U, V, W	dimensional velocities in R, θ, ϕ
W_a	average velocity

Dimensionless groups

De	Dean number based on apparent viscosity (Oliver and Ashar [24])
Gz	Graetz number based on apparent viscosity (Oliver and Ashar [24])
N_{De}	Dean number
N_{Gz}	Graetz number
N_{Nu}	Nusselt number
N_{Pr}	Prandtl number
N_{Re}	Reynolds number
N_{U_s}	Nusselt number in straight tube ($1.75Gz^{0.33}\delta_n^{0.33}$)

Greek letters

δ_n	$(3n+1)/4n$, correction factor to allow for velocity profile distortion due to pseudoplastic behaviour of liquid
δ	geometric parameter defined in Eq. (5E)
ϕ	axial co-ordinate
λ	curvature ratio
μ_p	consistency index
ν	$\mu_a/\rho = 8^{n-1}\mu_p$
o	defined in Eq. (8A)
O	dimension
θ	azimuthal co-ordinate
ρ	density of the fluid
ω	vorticity
ψ	nondimensional stream function
Ψ	dimensional stream function

Newtonian and non-Newtonian fluids in the thermal entrance region of straight tubes for different boundary conditions (Shah and Bhatti [32]). In contrast, practically no attention has been paid to the thermal entrance region of coiled tubes. Only the experimental study of Oliver and Ashar [24] has suggested forced laminar convection of a power law fluid in the thermal entrance region with a constant wall temperature. They correlated their heat transfer data for viscoelastic polyacrylamide solutions in different coils by using the modified Graetz Leveque equation.

The present paper presents a complete numerical solution for fully developed laminar flow and heat transfer for power law fluids in coiled tubes with a uniform wall temperature. The analysis sheds light on the interactions between the secondary flow and the developing temperature field for power law fluids. The Navier–Strokes equations in stream function/vorticity form are solved numerically by the successive over-relaxation method, and heat transfer equations are solved using an alternative implicit direction method. The numerical solutions are obtained for the case of steady-state, fully developed forced laminar convection of isothermal, incompressible power law fluids in the thermal entrance region of coiled tube within a rigorously treated toroidal geometry. The computations for fully developed laminar flow of power law fluids have been carried out over a wide range of system parameters such ash $1 < N_{De} < 500$, $5 < \lambda < 100$ and $0.5 < n < 1.5$. The numerical solutions for developing temperature profiles and average local Nusselt numbers include the range of $N_{De} < 100$, $0.7 < n < 1.5$ and $N_{Pr} < 50$. The numerical values of friction factors for different Reynolds numbers and curvature ratios along with the results for Nusselt numbers at different Graetz and Prandtl numbers are computed for Newtonian fluids as a special case. These calculations for Newtonian fluids were in good agreement with published theoretical and experimental results (Hsu and Patankar [13]).

2. Mathematical formulation

A representation of a coiled tube and its co-ordinate system is shown in Fig. 1. The toroidal geometry is a good approximation for helically coiled tubes of a small pitch.

In order to determine the heat transfer of power law fluids in coiled tubes, the equations of continuity, momentum

Table 1
Theoretical studies for the flow phenomena of power law fluids

S. no.	Name of investigator	Theoretical method	Range of parameters			Remarks
			Curvature ratio (λ)	Power law index (n)	Dean no. N_{De}	
1	Rathna [27]	Analytical method (perturbation method) solution is obtained upto first order term	20–100	0.5–1.5	1–20	Followed Dean's constraint, flow rate is independent of curvature ratio
2	Mashelkar and Devarajan [19]	Boundary layer approach	10–100	0.5–1.0	>50	Theory is applicable for higher values of Dean number. The theoretical correlation for friction coefficient (f_c) is given in Table 2
3	Hsu and Patnaker [13]	Numerical finite difference technique described by Patanker [25]	–	0.5–1.25	1–100	Followed Dean constraint. This analysis is applicable when curvature ratio is large
4	Takami et al. [34]	Numerical time marching method	10–100	0.5–1.0	1–1000	The relation f_c and N_{De} can be expressed with single curve which is dependent on n
5	Agarwal et al. [1]	Analytical perturbation method. Solution is found upto the second order term	10–100	0.5–1.5	1–30	Relaxing Dean's constraints and the flow rate is found a function of curvature ratio, Reynolds number and power law index
6	Kewase and Young [17]	Integral momentum boundary layer method	10–100	0.5–1.0	>100	The theory in applicable for both laminar and turbulent flow and heat transfer of power law fluids for high Dean number (N_{De} > 100)

Table 2
Experimental studies for the flow phenomena of power law fluids[a]

S. no.	Name of investigator	System (fluid)	Range of parameters			Correlation	Remarks
			λ	n	N_{De}		
1	Rejasekharan et al. [28]	CMS of 0.5 & 1% sodium silicate	30–100	0.8–10	10–2000	$F_c/f_s = 1.25\ (N_{De})^{0.3}$	Correlation does not reduce to Newtonian fluid
2	Gupta and Mishra [11,12]	CMC 0.6–2.1%	30–40	0.77–0.85	$1–10^4$	$F_c/f_s = 1 + 0.026\ (N_{De})^{0.675}$	Correlation is independent of power law index
3	Mujawar and Raja Rao [22]	SA SCMC 0.5–1.0%	10–100	0.7–1.0	$1–10^3$	$M = Re_{genc}(\lambda)^{m'_c}$, $Re_{genc} = \frac{dn'_c W_a^{(2-n'_c)}\rho}{g_c K'_c 8^{(n'_c-1)}}$ where K'_c, m'_c and n'_c are defined in terms of n and consistency index (μ_p)	Introduced dimensionless parameters M which characterize the flow phenomena of power law fluid in curved tube
4	Mashelker and Devarajan [20]	CMC PE PAA kaolan suspension	10–100	0.7–1.0	70–400	$F_c = (9.069 - 9.438n + 4.374n^2)(\lambda)^{-0.5} N_{De}{}^{(0.768+\ 0.122n)}$	The correlation predicts lower value of f_c for Newtonian fluids ($n = 1$) as predicted by White [38] equation
5	Takami et al. [35]	PAA PEO CMC	30–150	0.6–1.0	l–10^4	–	F_c/f_s is a function of N_{De} only and it does not depend on the value of n and curvature ratio
6	Mishra and Gupta [21]	CMC SCMC	30–150	0.7–1.0	$1–10^5$	$f_c/f_s = 1 + 0.033\ (\log N_{De})^{0.4}$	Study for turbulent flow of power law fluid
7	Singh and Mishra [33]	Water, starch 2–4%, CMS 2%, 3%	30–100	0.8–1.0	$1–10^4$	–	Laminar and turbulent flow of Newtonian and non-Newtonian fluids flowing through Archimedian spiral coils

[a] CMC: carboxy methyle cellulose; SCMS: sodium carboxy methyle cellulose; Sa: sodium alginate; Peo: polyethylene oxide; PAA: polyacrylamide.

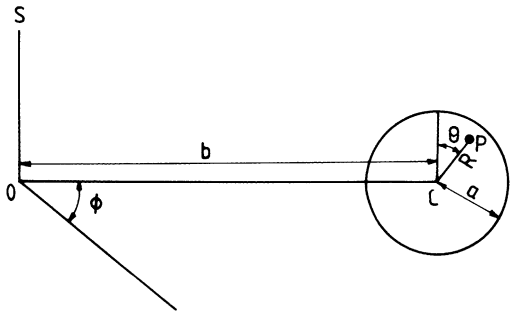

Fig. 1. To roidal co-ordinate system.

and energy must be solved. The following assumptions are made:

1. The flow is steady and fully developed.
2. The fluid is incompressible and obeys a power law.
3. The wall temperature is uniform.
4. The physical properties of fluids are constant and free convection is negligible.
5. Viscous dissipation is negligible and heat sources do not exist.
6. The axial conduction term is negligible compared with the radial conduction terms in the energy equation.

The nondimensional equations of the axial velocity w, the vorticity ω, the stream function Ψ of the secondary flow and the energy equations for the power law fluids under the proposed model are given below:

1. Axial momentum equation:

$$O\frac{\partial^2\omega}{\partial r^2}+\frac{\partial\omega}{\partial r}\left(\frac{\partial O}{\partial r}+\left(A+\frac{1}{r}\right)O-u\right)+\frac{\partial w}{\partial\theta}\left(\frac{1}{r^2}\frac{\partial O}{\partial\theta}+\frac{BOv}{r^2}\right)+O\frac{\partial^2 w}{r^2\theta^2}-w\left(\frac{O}{\lambda^2\delta^2}+Bv+Au+A\frac{\partial O}{\partial r}+\frac{B}{r}\frac{\partial O}{\partial\theta}\right)=\frac{1}{\lambda\delta}\frac{\partial p}{\partial\phi} \quad (1)$$

2. Vorticity transport equation:

$$O\frac{\partial^2\omega}{\partial r^2}+\frac{\partial\omega}{\partial r}\left(\frac{\partial O}{\partial r}+\left(A+\frac{1}{r}\right)O-u\right)+\frac{\partial\omega}{\partial\theta}\left(\frac{1}{r^2}\frac{\partial O}{\partial\theta}+\frac{BOv}{r^2}\right)+O\frac{\partial^2\omega}{r^2\partial\theta^2}-\left(\frac{O}{\delta^2\lambda^2}-(Bv+Au)\right)\omega+2w\left(B\frac{\partial w}{\partial r}-\frac{A}{r}\frac{\partial w}{\partial\theta}\right)+f_w=0 \quad (2)$$

3. Stream function vorticity equation

$$\lambda\delta\omega=\frac{\partial^2\psi}{\partial r^2}+\frac{1}{r^2}\frac{\partial^2\psi}{\partial\theta^2}+\left(\frac{1}{r}-A\right)\frac{\partial\psi}{\partial r}-\frac{B}{r}\frac{\partial\psi}{\partial\theta} \quad (3)$$

4. Energy equation:

$$N_{Pr}\left[\frac{\omega}{\delta}\frac{\partial T}{\partial\phi}\right]=\left[\frac{\partial^2 T}{\partial r^2}+\frac{1}{r^2}\frac{\partial^2 T}{\partial\theta^2}+\frac{1}{r}\frac{\partial T}{\partial r}+A\frac{\partial T}{\partial r}+\frac{B}{r}\frac{\partial T}{\partial\theta}\right]-N_{Pr}\left[u\frac{\partial T}{\partial r}+\frac{v}{r}\frac{\partial T}{\partial\theta}\right] \quad (4)$$

where

$$O=\left[\frac{1}{2}(e_{rr}^2+e_{\theta\theta}^2+e_{r\theta}^2+e_{\theta\phi}^2+e_{\phi r}^2)\right]^{(n-1)/2} \quad (5A)$$

$$e_{rr}=2\frac{\partial u}{\partial r}$$

$$e_{\theta\theta}=2\left(\frac{1}{2}\frac{\partial v}{\partial\theta}+\frac{u}{r}\right) \quad (5B)$$

$$e_{\phi\phi}=2(uA+vB)$$

$$e_{r\phi}=\left(\frac{\partial w}{\partial r}-Aw\right)$$

$$e_{r\theta}=\frac{\partial v}{\partial r}-\frac{v}{r}+\frac{1}{r}\frac{\partial u}{\partial\theta} \quad (5C)$$

$$e_{\theta\phi}=\frac{1}{r}\frac{\partial w}{\partial\theta}-Bw$$

$$f_w=\left(\frac{\partial O^2}{\partial r^2}-\frac{1}{r^2}\frac{\partial O^2}{\partial\theta^2}\right)e_{r\theta}+\frac{1}{r}\frac{\partial^2 O}{\partial\theta\partial r}(e_{\theta\theta}-e_{rr})+\frac{\partial O}{\partial r}\left[\frac{\partial e_{r\theta}}{\partial r}+\frac{1}{r}\frac{\partial e_{\theta\theta}}{\partial\theta}+\left(A+\frac{1}{r}\right)e_{r\theta}+B(e_{\theta\theta}-e_{\phi\phi})\right]-\frac{1}{r}\frac{\partial O}{\partial\theta}\left[\frac{\partial e_{rr}}{\partial r}-\frac{1}{r}\frac{\partial e_{r\theta}}{\partial\theta}+A(e_{rr}-e_{\phi\phi})-Be_{r\theta}\right] \quad (5D)$$

$$u=-\frac{1}{r\delta}\frac{\partial\psi}{\partial\theta},\qquad v=\frac{\partial\psi}{\delta\partial r}$$

$$\delta=\frac{b}{a}+r\sin\theta$$

$$A=\frac{\sin\theta}{\delta\lambda},\qquad B=\frac{\cos\theta}{\delta\lambda} \quad (5E)$$

Eq. (1) for axial momentum and Eq. (4) for temperature are modified at $r=0$ by using L'Hospital rule because of their singularity.

$$O\frac{\partial^4\omega}{2\partial r^2\partial\theta^2}+2O\frac{\partial^2\omega}{\partial\theta^2}-w\times\left[\frac{O}{\delta^2}+Bv+Au+A\frac{\partial O}{\partial r}+\frac{\partial^2 O}{\partial r\partial\theta}\right]=\frac{1}{r}\frac{\partial p}{\partial\phi} \quad (6)$$

$$N_{Pr}\left[\frac{\omega}{\lambda\delta}\frac{\partial T}{\partial\phi}\right] = 2\frac{\partial^2 T}{\partial r^2} + \frac{\partial^4 T}{2\partial r^2\partial\theta^2} + B\frac{\partial^2 T}{\partial r\partial\theta} - N_{Pr}\left[v\frac{\partial^2 T}{\partial r\partial\theta}\right] \quad (7)$$

The above equations are nondimensionalised by introducing the following substitutions:

$$u, v, w = (U, V, W)\frac{\rho a^n}{\mu_p^{1/(n-2)}}$$

$$r = \frac{R}{a}$$

$$o = O\frac{\rho a^2}{\mu_p^{(n-1)/(n-2)}}$$

$$\psi = \Psi\frac{\rho a^{(3n-4)}}{\mu_p}$$

$$\omega = \Omega\frac{\rho a^2}{\mu_p^{1/(n-2)}} \quad (8A)$$

$$p = P\frac{\rho^n a^{2n}}{\mu_p^{1/(n-2)}}$$

$$T = \frac{(T^* - T^{\circ})}{(T_w - T^{\circ})}$$

The Reynolds and Prandtl numbers for power law fluids are defined in the following manner:

$$N_{Re} = \frac{\rho(W_a)^{2-n}d_t^n}{\mu_p},$$
$$N_{Pr} = \frac{\rho^{(n-1)/(n-2)}c_p a^{2(n-1)/(n-2)}}{\mu_p^{1/(n-2)}K_c} \quad (8B)$$

3. Boundary conditions

The following standard boundary conditions for constant wall temperature are used:

$$\omega(1,\theta) = 0, \qquad \frac{\partial\omega}{\partial r}(0,0) = 0$$

$$\frac{\partial\omega}{\partial\theta}\left(r, \pm\frac{\pi}{2}\right) = 0$$

$$\psi(1,\theta) = 0, \qquad \frac{\partial\psi}{\partial r}(1,\theta) = 0$$

$$\psi(0,0) = \psi\left(r, \pm\frac{\pi}{2}\right) = 0$$

$$\omega(1,\theta) = \frac{\partial^2\psi}{\delta\partial^2 r}(1,\theta) \quad (9)$$

$$\omega(0,0) = \omega\left(r, \pm\frac{\pi}{2}\right) = 0$$

$$\phi = 0, \qquad T = 0$$

$$\frac{\partial T}{\partial\theta}\left(r, \pm\frac{\pi}{2}\right) = 0$$

$$T(1,\theta) = 1$$

$$\frac{\partial T}{\partial r}(0,0) = 0$$

4. Method of solution

Eqs. (1)–(4) were numerically solved using finite difference scheme. The computations have been carried out only in the domain of the upper semi circular region of the tube cross-section due to the symmetry along the central plane. Standard second order central difference operators were used for the first and second derivative of w, ω, ψ and T in both the radial and angular directions.

The finite difference equations for w, ω and ψ were solved by a successive over-relaxation technique (Greenspan [10]). The energy Eq. (4) is somewhat analogous to the two dimensional unsteady-state heat conduction equation, and an alternative direction implicit (ADI) method transformed the energy Eq. (5) into a set of algebraic equations (Douglas and Gunn [7] and Peaceman and Rachford [26]). When second order central differences are used, the result is tri-diagonal system. This can be solved using the Thomas algorithm [37]. The steady-state values of u, v and w for a particular Reynolds number, power law index and curvature ratios were then used to calculate temperature profiles as a function of ϕ.

A detailed description of the computational procedure and criteria for stability and convergence are available elsewhere (Agrawal et al. [2]).

Once a complete convergent solution of velocities were obtained, values of the Reynolds numbers, Dean numbers and friction factors were computed for the particular value of axial pressure gradient, curvature ratio and power law index. The Reynolds numbers, Dean number and friction factors for power-low fluids in curved tube are

$$N_{Re} = \frac{2^n}{\pi}\left\{\int_0^{2\pi}\int_0^1 rw\,\mathrm{d}r\,\mathrm{d}\theta\right\}^{2n}$$

$$f_s = \frac{8\{2((3n+1)/n)\}^n}{N_{Re}} \quad (10)$$

$$f_c = 2^{(4/(2-n))}(N_{Re})^{(2/(n-2))}\left\{-\frac{1}{\lambda}\frac{\partial p}{\partial\phi}\right\}$$

$$N_{De} = \frac{N_{Re}}{\sqrt{\lambda}}$$

The computed values of temperature were used to obtain the peripherally averaged Nusselt and Graetz numbers:

$$N_{Nu}(\theta,\phi) = \frac{2}{(T_w - T_b(\phi))}\frac{\partial T}{\partial r}(1,\theta,\phi) \tag{11}$$

$$N_{Nu}(\phi) = \frac{N_{Re}N_{Pr}}{2\lambda(T_w - T_b)}\frac{\partial T}{\partial \phi}(\phi) \tag{12}$$

$$N_{Gz} = \pi\frac{N_{Re}N_{Pr}}{2\lambda\phi}$$

where T_b is the bulk temperature which is defined as

$$T_b(\phi) = \frac{\int_0^{2\pi}\int_0^1 Twr\,dr\,d\theta}{\int_0^{2\pi}\int_0^1 wr\,dr\,d\theta} \tag{14}$$

4.1. Axial velocity profiles

The patterns of axial velocity profile in horizontal and vertical plane for the power law fluids for different values of Dean number of 60 and 300 are shown in Fig. 2. These patterns of velocity profiles are compared to those of Takami et al. [34,35] and found to be in good agreement. Fig. 2 shows the influence of power law index, n, on the axial velocity profiles for given Dean number. As the pseudoplasticity increases, the viscous boundary layer becomes limited to the outer wall of the pipe and its thickness reduces as shown in Fig. 2. For dilatant fluids it can be seen that the viscous region becomes thicker and shifts towards the central region. The velocity profiles tend to flatten for the lower value of n, which is in conformity with the effect of n on the velocity profile in a straight tube. It can also be observed that, as the value of Dean number increases, the maximum velocity shifts more towards the outer wall for power law fluids.

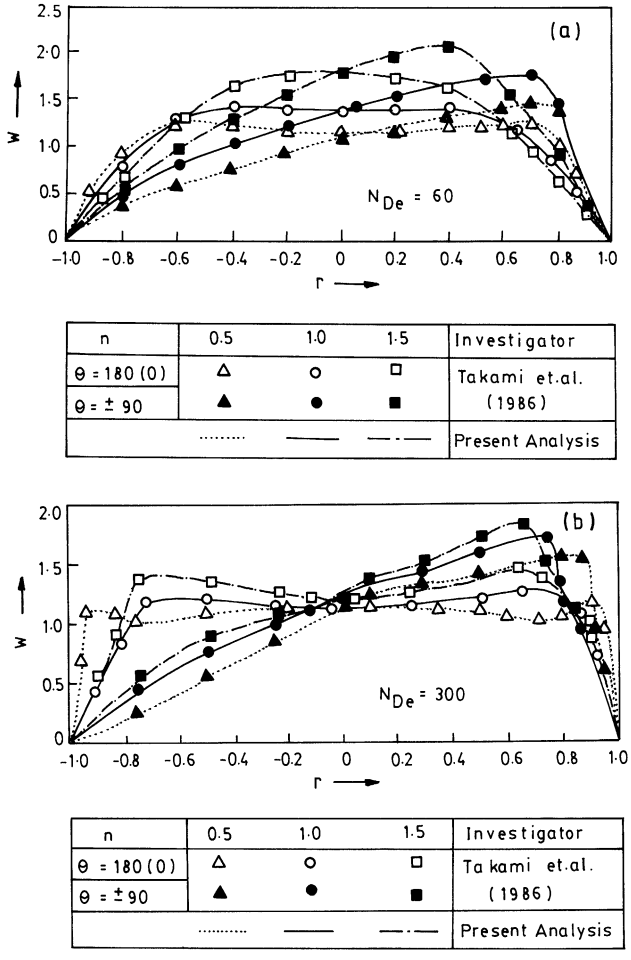

Fig. 2. Axial velocity profiles using numerical solutions.

4.2. Effect of power law index on f_c/f_s

The values of friction factor for Newtonian and power law fluids are shown in Fig. 3. For the Newtonian fluids, the friction factor results are compared with published theoretical and experimental results (Ito [14], White [38]). It is clear that the present analysis predicts the experimental data over a wide range of system parameters with a high degree of accuracy. Liu et al. [18] investigated experimentally the pressure drop of fully developed incompressible laminar Newtonian flow in helical coils of constant cross-section having a finite pitch. Their experimental results for zero pitch are found in good agreement with the published experimental results of Ito [14] and White [38]. Our present analysis is also able to simulate the experimental results of Liu et al. [18] for zero pitch. The dependence of power law index and Dean number on friction factor is shown in Fig. 3. For a given fluid, the friction factor increases with increases in Dean number, and for a given N_{De}, it decreases with increases in power law index. At a first glance it may appear that the present results are contradictory to the results of Hsu and Patankar [13]. However, this discrepancy is caused by to the difference in nondimensionalizing the equation of motion which makes the Reynolds number change by a factor C where C is $(8^n(3n+1)/4n)^n$. Individual values of friction factor for power law fluids are compared with the results of Hsu and Patankar [13] as shown in Fig. 3b and c. This difference may be attributed to the fact that the present analysis was carried out without introducing assumptions and simplifications of Dean's analyses [5,6] and it is expected to give more realistic predictions.

4.3. Comparison of f_c/f_s results with published results

The results for f_c/f_s for $n = 0.75$ and 0.82 were compared with the results of Hsu and Patankar [13], and with the data of Mujawar and Raja Rao [22] and Mashelkar and Devarajan [19,20]. The agreement of the computed results with the experimental data is good. It is relevant here to comment on the empirical correlations of f_c/f_s proposed previously. The correlation of Rajasekharan et al. [28] and Gupta and Mishra [11,12] and Takami et al. [34,35] express f_c/f_s as a function of Dean number only and do not account for the influence of n.

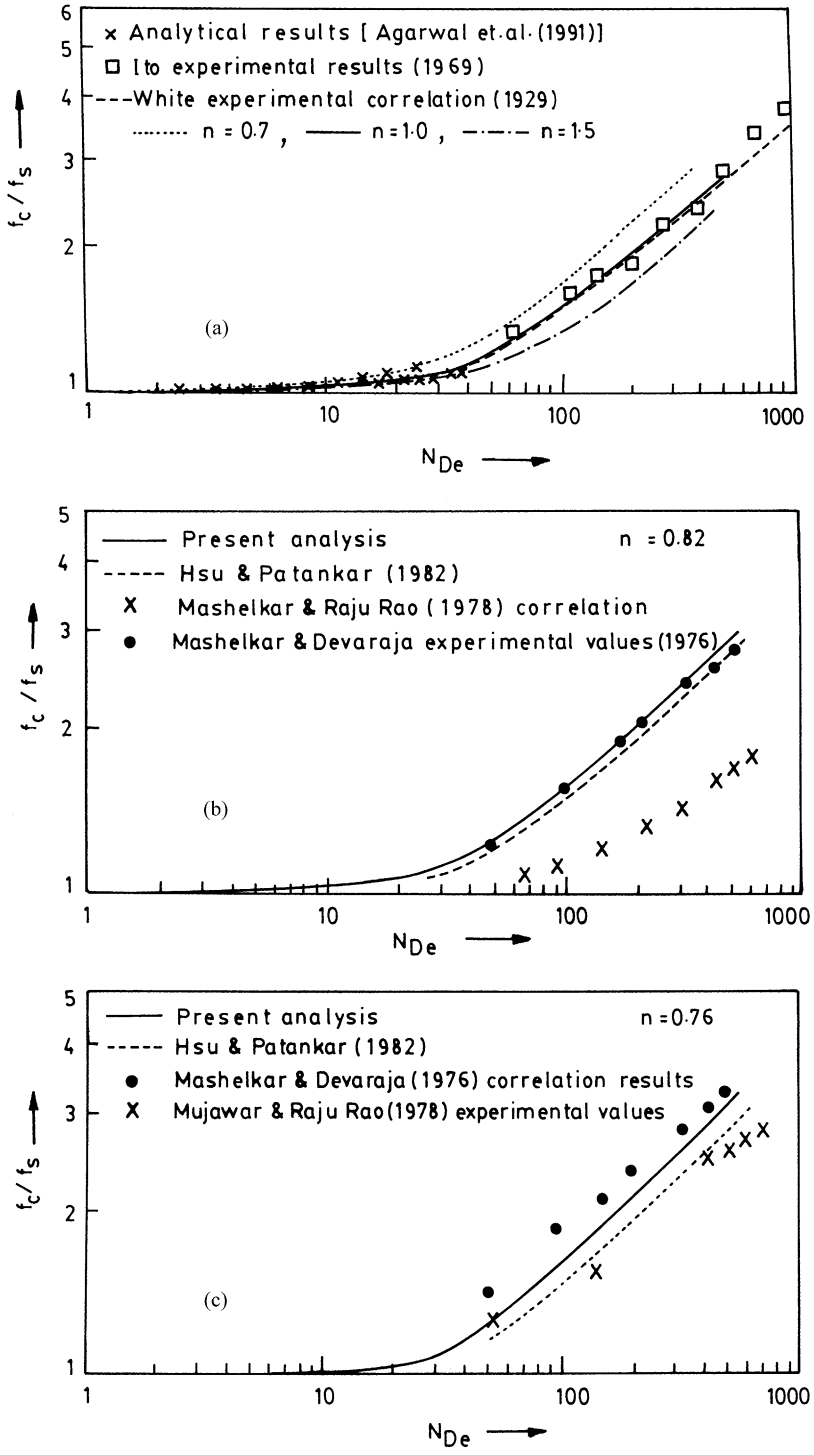

Fig. 3. (a) Variation of the friction factor ratio with N_{De} for different value of n; (b) and (c) comparison of the fully developed friction factors with the published results.

The correlation of Mashelkar and Devarajan [19,20] does not correctly describe the data for Newtonian flow in curved tube but the correlation described by them is a good design tool to calculate f_c/f_s for power law fluids as shown in Fig. 3b and c. The correlation given by Mujawar and Raja Rao [22] does not have these obvious shortcomings but as indicated in Fig. 3b and c, their data and their correlation tend to underestimate f_c/f_s values. These shortcomings were also reported by Hsu and Patankar [13]. Saxena and Nigam [30] have pointed out that the Mujawar and Raja Rao [22] dimensionless number (M) may not be a true representation of the hydrodynamics in the helical flow of power law

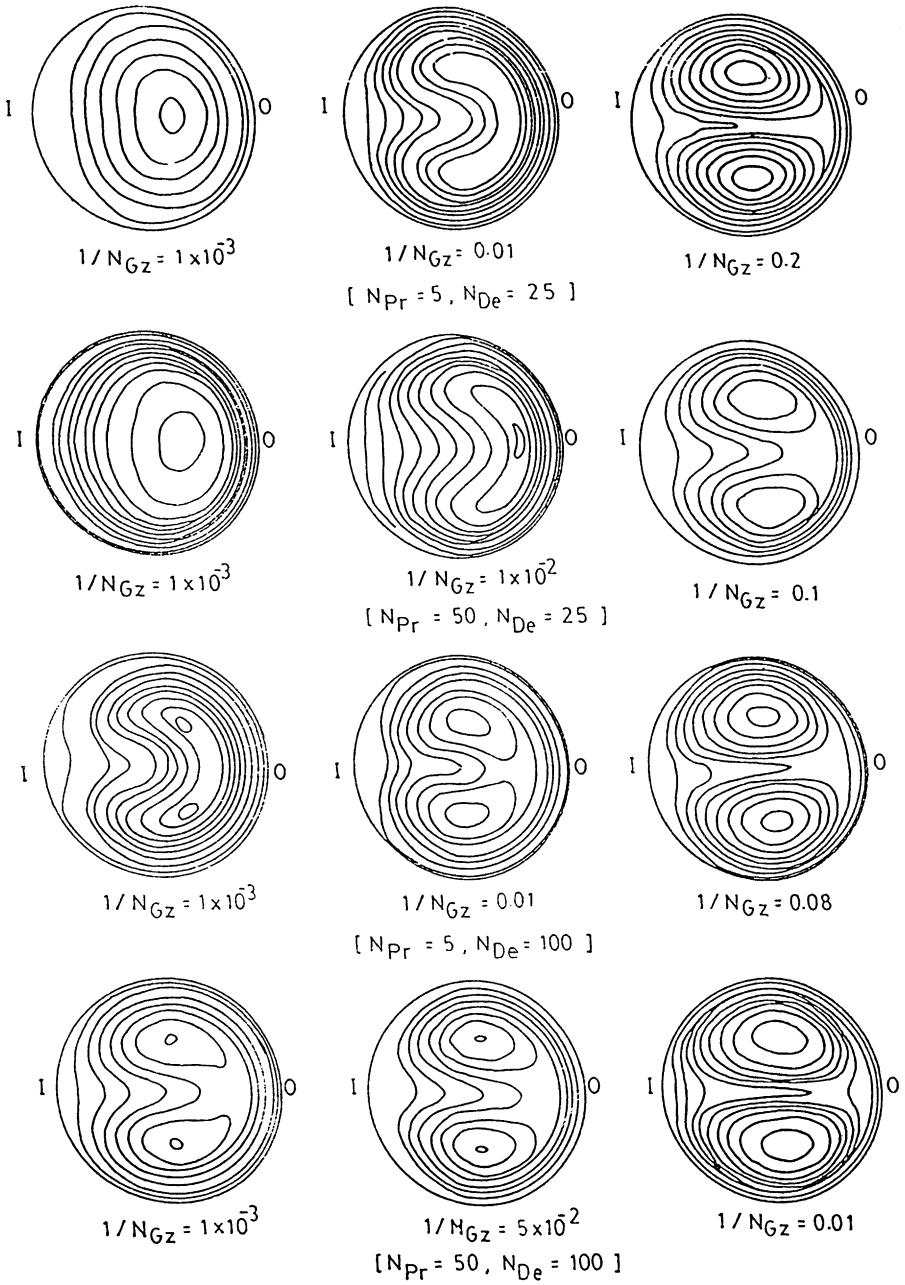

Fig. 4. Development of isotherms for different N_{De} and N_{Pr} at different axial positions ($1/N_{Gz}$) ($n = 0.7$). I: inner wall; O: outer wall.

fluids and is not useful for characterising axial dispersion in coils.

4.4. Development of temperature profiles

The interaction between the fully established secondary flow of power law fluids and the developing temperature fields in curved pipes represent a major departure from the classical Graetz [9] problem in straight tube. The development of the temperature profile may be understood by a study of the isotherms at different axial positions. Figs. 4 and 5 show the computed temperature profiles for different Prandtl and Dean numbers for $n = 0.7$ and 1.5 corresponding to pseudoplastic and dialtant behaviour, respectively. At different axial positions which are represented by $1/N_{Gz}$ number, the temperature fields have been plotted in the form of isotherms. For very short distance from the tube inlet ($1/N_{Gz}$ is $O(10)^{-4}$ to $O(10)^{-3}$) the secondary flow effect is negligible so the isotherm in a coiled tube is similar to that in straight tube. The secondary velocities increase very rapidly with increasing distance from the tube wall. Therefore, as the thermal boundary layer grows with

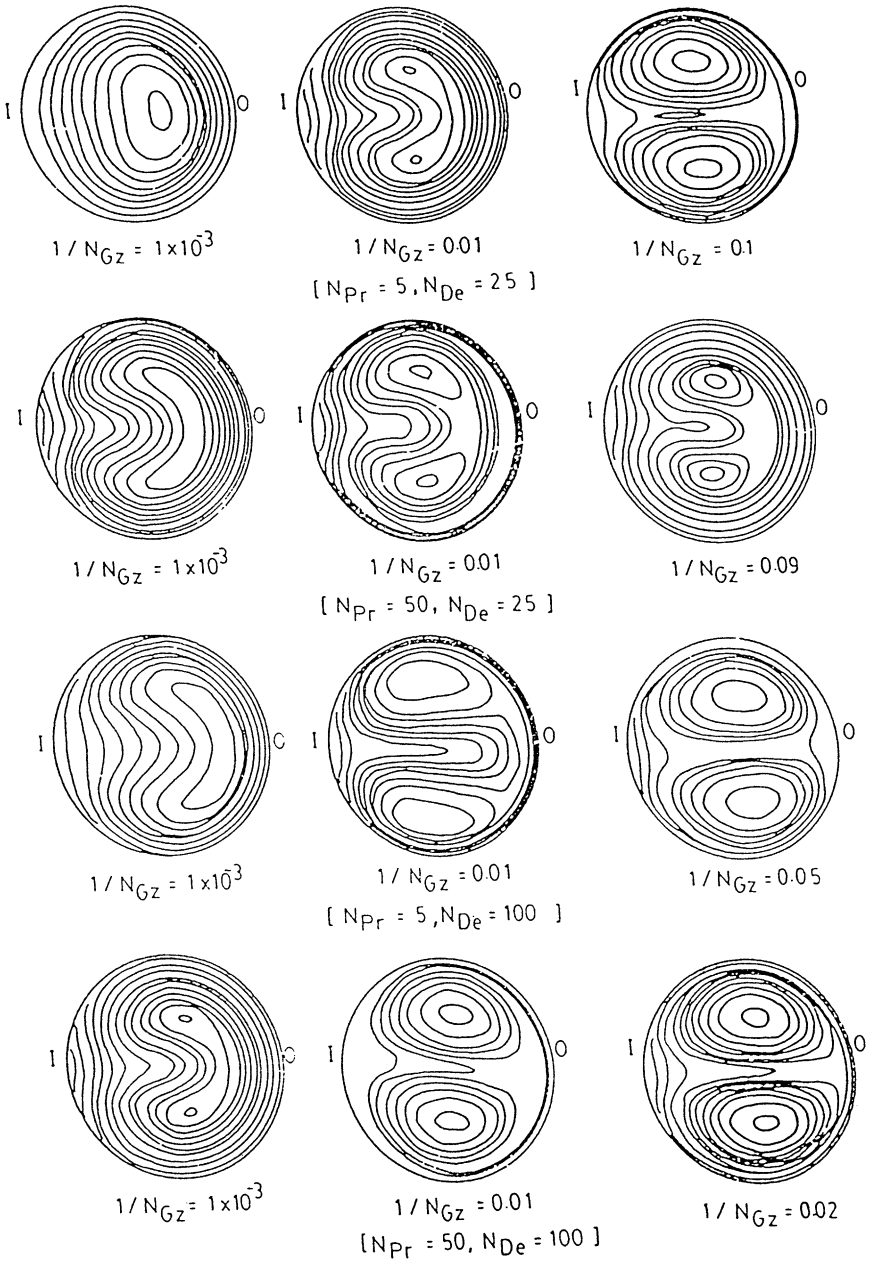

Fig. 5. Development of isotherms for different N_{De} and N_{Pr} at different axial positions ($1/N_{Gz}$) ($n = 1.5$). I: inner wall; O: outer wall.

advancing axial distance, the secondary convection of heat becomes pronounced. This temporarily arrests the growth of the thermal boundary layer and the secondary convection transfers much of the heat into the fluid core. Because of this effect the isotherms become kidney shaped and more skewed toward the outer wall of the tube. At a particular value of $1/N_{Gz}$ ($O(10)^{-2}$ to $O(10)^{-1}$) the isotherms appear in two cell pattern. As the temperature profile approaches to the fully developed stage the isotherms line up with the secondary flow and the two closed contours of isotherms are found to be symmetrical about the plane of the curvature of the coil. The change in pattern of developing temperature profiles for different power law fluids are discussed later.

4.5. Variation of Nusselt numbers in the thermal entrance region

Figs. 6 and 7 display the behaviours of the circumferential averaged local Nusselt number for power law fluids as a function of various Dean and Prandtl numbers. The variation of the local Nusselt numbers in the thermal entrance region is of considerable importance to basic understanding of heat transfer in coiled tubes. The use of two alternative expressions (Eqs. (11) and (12)) in evaluating the local Nusselt numbers is particularly useful in checking the accuracy of numerical results. The values found using these two expressions show a maximum deviation of 1.5% from the average

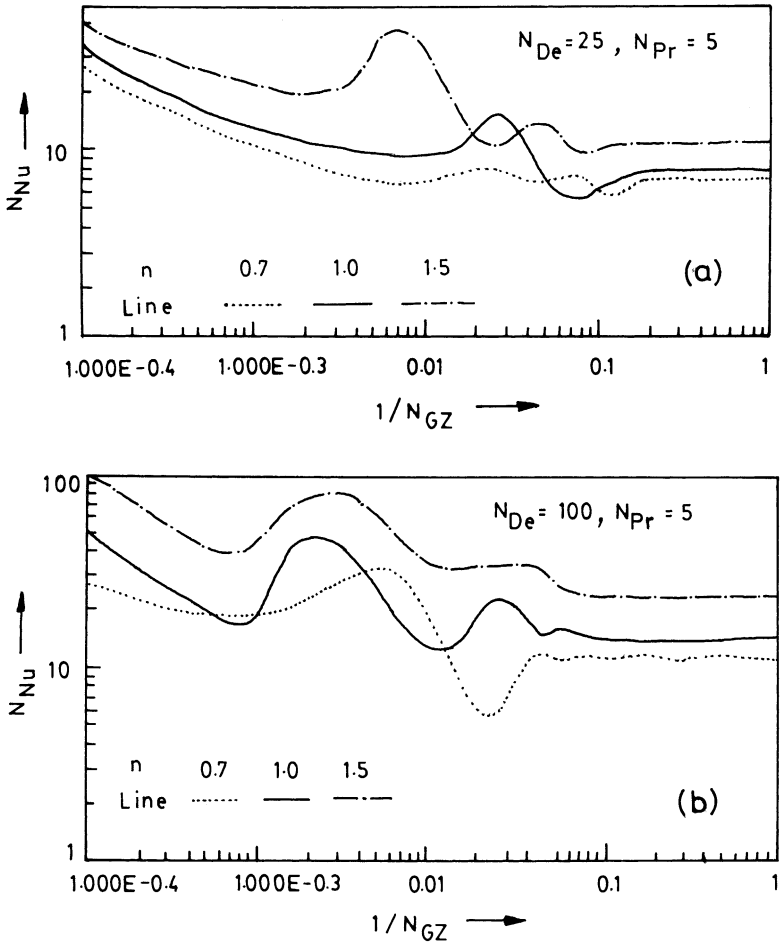

Fig. 6. Effect of power law index on local Nusselt number variations along the axial distance for $N_{Pr} = 5$.

values, indicating good convergence and accuracy. The Nusselt number variations are closely related to the isotherms at various axial distances. The oscillatory character of the Nusselt numbers is due to the circulatory secondary flow. One direct consequence of the circulation is a sudden decrease in temperature gradient at the tube wall and therefore a decrease in heat transfer coefficient. The cyclic variations damp out as the fully developed temperature field is approached and the Nusselt number approaches an asymptotic value. Increasing the Dean number is seen to increase the Nusselt number and shorten the thermal entrance length. Figs. 6 and 7 show that the intensity of the cyclic behaviour of Nusselt number increases with increase in N_{Pr} and N_{De}. This is due to the increase in the intensity of the secondary convection. It may also be concluded from Figs. 6 and 7 that the thermal entry length is mainly influenced by thermal diffusivity.

It is clear from the Figs. 6 and 7 that the asymptotic values of Nusselt number decrease with power law index for a given Prandtl and Dean numbers. The thermal entrance length also increases with decreases in power law index at a particular value of Dean and Prandtl numbers. This phenomena is due to the effect of secondary flow of power law fluids. The intensity of secondary flow in power law fluids decreases with increasing pseudoplasticity of the fluids (Takami et al. [34,35], Hsu and Patankar [13] and Agrawal et al. [1]). The power law constitutive equation reveals that the pseudoplastic fluids ($n < 1$) sustain less strain and dilatant fluids ($n > 1$) sustain more strain than Newtonian fluids. Therefore, as the pseudoplasticity of the fluids increases, the effect of convection becomes less and hence the velocity profiles become more blunt which causes a decrease in the intensity of secondary flow. The weak intensity of secondary flow in pseudoplastic fluids increases the length of the thermal entrance region.

4.6. Asymptotic Nusselt number

The asymptotic values of numerically computed Nusselt number for Newtonian fluids are compared with published results of Dravid et al. [8], Akiyama and Cheng [3]; Hsu and Patankar [13] as shown in Table 3. The comparison is good. Some discrepanices may occur due to the difference in the boundary conditions as constant flux was assumed by Hsu

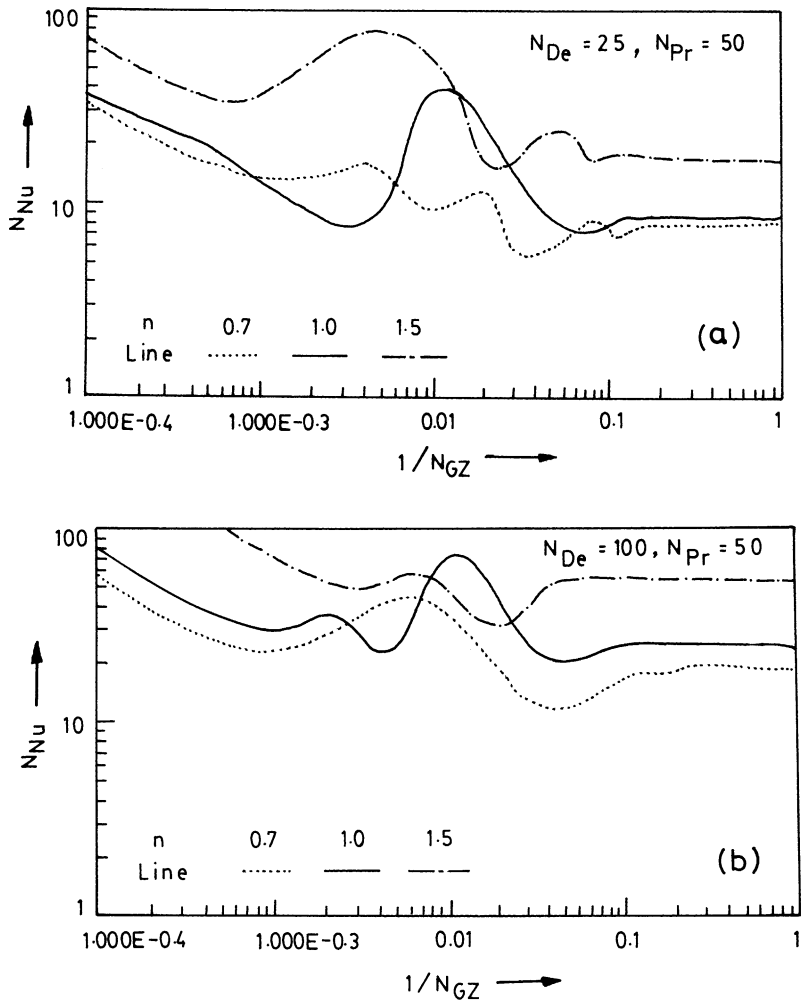

Fig. 7. Effect of power law index on local Nusselt number variations along the axial distance for $N_{Pr} = 50$.

and Patankar [13]. The asymptotic values of Nusselt number for power law fluids are compared with those of Hsu and Patankar [13] in Table 4. For given Prandtl and Dean numbers the asymptotic Nusselt number increases with increases in the power law index. The Nusselt number also increases with increases in Dean number and Prandtl number for given power law fluid. Table 4 also confirmed the conclusion of Janssen that the over all heat transfer coefficient for the cases of constant wall temperature and constant wall heat flux are similar.

4.7. Comparison of heat transfer results with experimental result

The present analysis is compared with the Janssen and Hoogendoorn's [16] experimental data and correlation as shown in Fig. 8. Their experimental results followed the oscillating curve for very short tube lengths. For the thermal entrance region they derived the empirical correlation which predicted the results within 20% deviation. It is clear from the Fig. 8 that the present analysis is able to simulate the

Table 3
Comparison of asymptotic Nusselt numbers of Newtonian fluids with published results

N_{De}	N_{Pr}	Dravid et al. [8]	Hsu and Patankar [13]	Akiyama and Cheng [3]	Present analysis
50	5	7.098	8.94	–	8.98
	10	8.91	10.91	11.1	11.7
	50	10.62	17.45	–	18.21
100	5	9.62	12.21	–	11.9
	10	10.86	16.58	17.30	17.39
	50	14.40	23.12	–	25.04

Table 4
Comparison of asymptotic Nusselt number of power law fluids with Hsu and Patankar result [13]

N	N_{De}	N_{Pr}	Values of asymptotic Nusselt number	
			Present analysis	Hsu and Patankar analysis [13]
0.5	25	5	7.25	6.64
		15	8.10	7.83
		30	10.03	9.49
	50	5	8.30	7.59
		15	10.55	9.25
0.75	50	5	9.23	8.75
		15	11.50	10.35
		30	12.85	12.25
		50	15.60	14.85
	100	5	12.05	11.25
		15	14.50	12.15
		30	16.55	14.85
		50	20.22	17.10
1.25	75	5	15.90	15.39
		15	22.10	21.80
		30	26.80	25.08
		50	32.20	31.21
	100	5	20.95	20.52
		15	24.12	23.60
		30	30.50	29.93
		50	37.20	30.37

oscillating nature of the experimental results in the thermal entrance region and is in reasonably good agreement with their empirical correlation:

$$N_{Nu} = (0.32 + 3\lambda^{-1}) N_{Re} N_{Pr} \left(\frac{d}{z}\right)^{0.34+0.8\lambda^{-1}} \quad (14a)$$

For $2.0 < N_{De} < 8.3 \times 10^2$,
$30 < N_{Pr} < 4.5 \times 10^5$ and $10^{-2} < \lambda^{-1} < 8 \times 10^{-2}$ (14b)

Before comparing the experimental results of Oliver and Ashar [24] with our numerical model, it is essential to understand how they have characterized the phenomena of heat transfer of power law fluids in thermal entrance region of circular curved tube. They correlated N_{Nu} as a function of power law index, Dean number and Graetz number. The effect of temperature on apparent viscosity was included by group $(\nu_w/\nu_b)^{0.14}$ in the correlations. Our model for heat transfer of power law fluids in the thermal entrance region is characterised by Dean number, Prandtl number, Graetz number and power law index. The effect of temperature on apparent viscosity was not considered. The experimental study did not consider Prandtl number as an independent variable because of its dependence on the Graetz number. The values of Dean number, Prandtl number and Graetz number in the

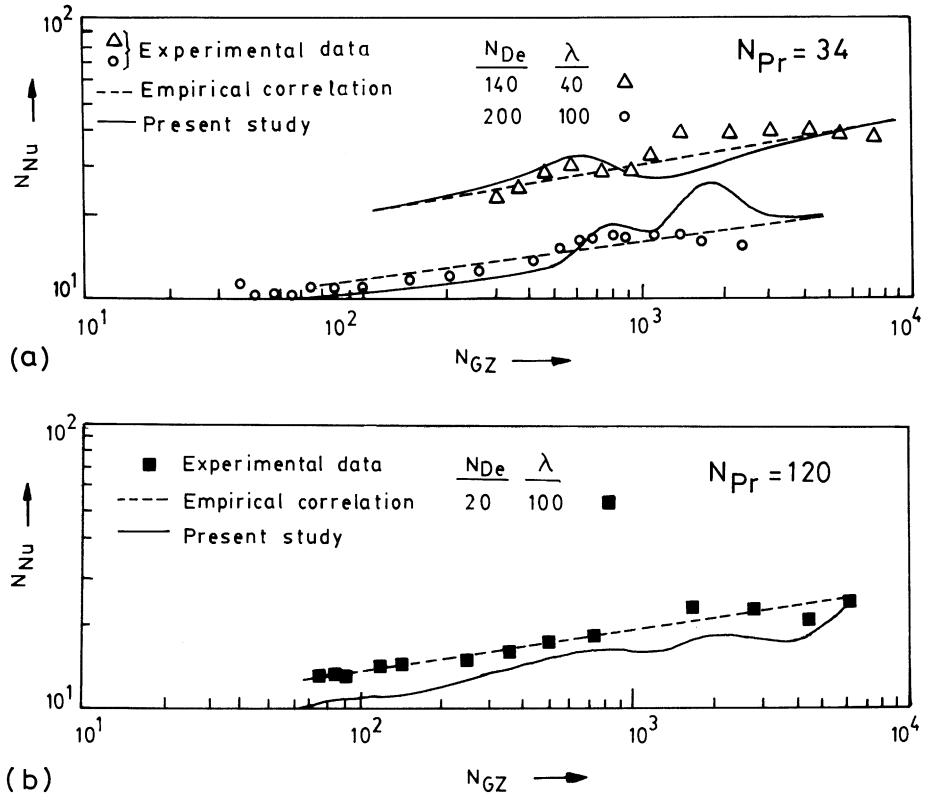

Fig. 8. Comparison of present study with experimental data of Janssen and Hoogendoom [16].

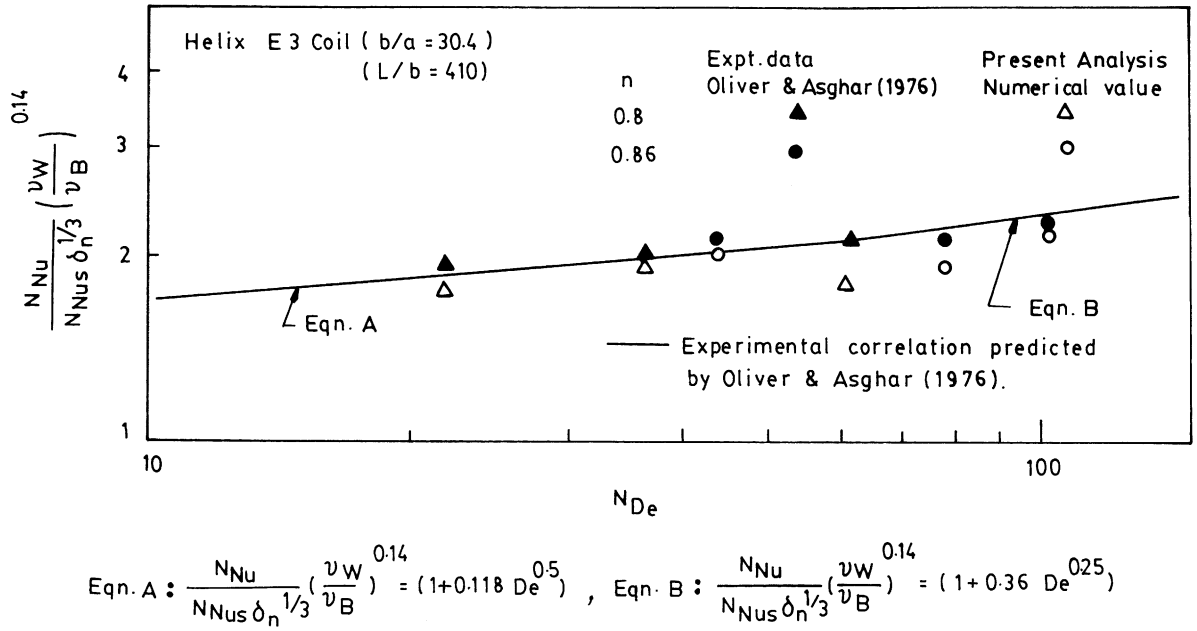

Fig. 9. Comparison of numerical results with experimental correlation predicted by Oliver and Asghar [24].

experimental analysis were computed by using the expression of apparent viscosity based on a straight tube geometry. The experimental values of Nusselt number were calculated on the basis of logarithmic mean temperature over the length of the tube. Oliver and Ashar [24] measured heat transfer and correlated their data by using the modified Graetz Leveque equation. The resulting correlations are

$$N_{Nu}\left(\frac{\nu_w}{\nu_b}\right)^{0.14} = 1.75\delta_n^{0.33}Gz^{0.33}(1+0.118De^{0.5}),$$
$$60 < De < 2000 \qquad (15a)$$

$$N_{Nu}\left(\frac{\nu_w}{\nu_b}\right)^{0.44} = 1.75\delta_n^{0.33}Gz^{0.33}(1+0.36De^{0.25}),$$
$$4 < De < 60 \qquad (15b)$$

Fig. 9 shows the comparison of numerical results of power law fluids ($n = 0.8$ and 0.86) for different values of Dean number with the experimental correlation of Oliver and Ashar [24]. As suggested by Oliver and Ashar [24], the values of $(N_{Nu}/N_{U_s}\delta_n^{1/3})(\nu_w/\nu_b)^{0.14}$ have been plotted for different values of Dean number (N_{De}) in Fig. 9. The solid line in Fig. 9 presents the experimental correlation Eqs. (15a) and (15b) values of $(N_{Nu}/N_{U_s}\delta_n^{1/3})(\nu_w/\nu_b)^{0.14}$ for different Dean number and the symbols and (●) represent the numerically computed values for $n = 0.8$ and $n = 0.86$, respectively. It may be concluded from Fig. 9 that the effect of secondary convection in curved tube enhanced the heat transfer by the factor of 1.5–2.0 with corresponding to straight tube for the same values of Reynolds, Prandtl and Graetz number. Therefore, the coils offer considerable advantage over straight tube from the point of view of laminar heat transfer of power law fluids.

5. Conclusions

The purpose of this paper is to present a complete numerical solution for the Graetz problem in coiled tubes for power law fluids with uniform wall temperature valid upto $N_{De} < 100$, $N_{Pr} < 50$ and $0.7 < n < 1.5$. The interaction between the effect of secondary flow of power law fluids and developing temperature profiles have shed some light on the phenomena of heat transfer in the thermal entrance region of circular curved tube. The following conclusions may be drawn for the phenomena of fully developed laminar flow and forced convection in thermal entrance region of laminar flow of power law fluids flowing through circular curved tubes:

1. The secondary flow becomes weak as the power law index decreases, but its dependence on Dean number is similar to that of Newtonian fluids.
2. The axial velocity is distorted by centrifugal forces, although it tends to flatten as the pseudoplasticity of the fluid increases.
3. The friction factor for power law fluids increases with increases in Dean number. For a given value of Dean number the value of friction factor increases with increases in power law index.
4. The Graetz problem of power law fluids flowing through curved circular tubes is characterised by the secondary flow effect superimposed upon the usual thermal entry

effect. Due to the effect of secondary flow the Nusselt number does not decrease continuously with axial distance, but undergoes cyclic oscillations with axial distance. These oscillations damp out as the region of fully developed temperature fields are approached.

5. At a particular value of Dean number of power law fluids, the increase in value of the Prandtl number is to shorten the thermal entrance length. As Prandtl number increases the temperature fields develops rapidly. The effect of Dean number is similar to that of Prandtl number for a given power law fluid.
6. The thermal entrance length increases with increase in pseudoplasticity of the fluid for a given Dean number and Prandtl number. At a particular value of Dean and Prandtl number the values of Nusselt number increase with increase in the values of power law index.

Acknowledgements

S. Agrawal wishes to thank Centre for Scientific and Industrial Research for financial Support to carry on the research.

References

[1] S. Agrawal, G. Jayaraman, V.K. Srivastava, K.D.P. Nigam, Power law fluids in circular curved tube. Part I. Laminar flow, Polym. Plast. Technol. Eng. 32 (1993) 595–614.
[2] S. Agrawal, Ph.D. Thesis, Indian Institute of Technology, Delhi, India, 1994.
[3] M. Akiyama, K.C. Cheng, Laminar forced convection with thermal entrance region of curved tube with uniform wall temperature, Can. J. Chem. Eng. 52 (1974) 234–240.
[4] S.A. Berger, L. Talbot, L.S. Yao, Flow in curved pipes, Ann. Rev. Fluids Mech. 15 (1983) 461–512.
[5] W.R. Dean, Note on the motion of fluid in a curved pipe, Philos. Mag. 4 (1927) 208–223.
[6] W.R. Dean, The stream-line motion of fluid in a curved pipe, Philos. Mag. 4 (1928) 673–685.
[7] J. Douglas, J.E. Gunn, A general formulation of alternating direction methods. Part 1. Parabolic problems, Numerische Mathematik 6 (1964) 428–453.
[8] A.N. Dravid, K.A. Smith, E.W. Merrill, P.L.O. Brian, Effect of secondary fluids motion on laminar flow heat transfer in helically coiled tubes, AIChE J. 17 (1921) 1114–1122.
[9] L. Graetz, Uber Die Warmeleitumgsfahigked van Flursigkeiten, Ann. Physik. Chemie 25 (1885) 1337–1345.
[10] D. Greenspan, Introductory Numerical Analysis of Elliptic Boundary Value Problems, Harper & Row, New York, 1965.
[11] S.N. Gupta, P. Mishra, Isothermal laminar flow of non-Newtonian fluids through helical coils, Indian J. Tech. 13 (1975) 245–250.
[12] S.N. Gupta, P. Mishra, Laminar forced convection heat transfer in non-Newtonian fluids in helical coils, in: Proceedings of the 3rd National Heat Mass Transfer Conference, Vol. 1, Indian Institute of Technology, Bombay, India, 1975, pp. 13–17.
[13] C.F. Hsu, S.V. Patankar, Analysis of laminar non-Newtonian flow and heat transfer in curved tubes, AIChE J. 28 (4) (1982) 610–616.
[14] H. Ito, Flow in curved pipes, Z. Angrew Math. Mech. 49 (1969) 653–663.
[15] H. Ito, Flow in curved pipes, JSME J. 30 (1987) 543–552.
[16] L.A.M. Janssen, C.J. Hoogendoorn, Laminar convection heat transfer in helically coiled tube, Int. J. Heat Mass Transfer 21 (1978) 1197–1206.
[17] Y. Kewase, M.M. Young, Momentum and heat transfer in non-Newtonian fluids flowing through coiled tubes, Ind. Eng. Chem. Res. 26 (6) (1987) 1248–1254.
[18] S. Liu, A. Artin, A. Nasr-El-Din Hisham, H.M. Jacob, An experimental study of pressure drop in helical pipes, Proc. R. Soc. Lond. A 444 (1994) 307–316.
[19] R.A. Mashelkar, G.V. Devarajan, Secondary flow of non-Newtonian fluids. Part 1. Laminar boundary layer flow of a generalized non-Newtonian fluids in a coiled tube, 54 (1976a) 100–107.
[20] R.A. Mashelkar, G.V. Devarajan, Secondary flow of non-Newtonian fluids. Part 2. Frictional losses in laminar flow of purely viscous and viscoelastic fluids through coiled tubes, Trans. Inst. Chem. Eng. 54 (1976) 108–114.
[21] P. Mishra, S.N. Gupta, Momentum transfer in curved pipes. Part 2. Non-Newtonian fluids, Ind. Eng. Chem. Process Des. Dev. 18 (1979) 137–142.
[22] B.A. Mujawar, M. Raja Rao, Flow of non-Newtonian fluids through helical coils, Ind. Eng. Chem. Process Des. Dev. 17 (1) (1978) 22–27.
[23] R.K. Nandakumar, J.H. Masliyah, Swirling flow and heat transfer in coiled and twisted pipes, in: A.S. Mujumdar, R.A. Mashelkar (Eds.), Advances in Transport Processes, Wiley, New Delhi, 1986, pp. 49–112.
[24] D.R. Oliver, S.M. Ashar, Heat transfer in Newtonian and viscoelastic liquids during laminar flow in helical coils, Trans. Inst. Chem. Eng. 54 (1976) 218–224.
[25] S.V. Patankar, Numerical Heat Transfer and Fluid Flow, McGraw-Hill, New York, 1980.
[26] D.W. Peaceman, H.H. Rachford, The numerical solution of parabolic and elliptic differential equation, J. Soc. Ind. Appl. Math. 3 (1955) 28–412.
[27] S.L. Rathna, Flow of a power law fluid in a curved pipe of circular cross-section, in: Proceedings of the Fluid Mechanical Symposium, Indian Institute of Science, Bangalore, 1967, pp. 378–388.
[28] S. Rajasekharan, V.G. Kubair, N.R. Kuloor, Flow of non-Newtonian fluids through helical coils, Indian J. Tech. 8 (1970) 379–391.
[29] K.K. Raju, S.L. Rathna, Heat transfer for the flow of power law fluids in a curved pipe, J. Indian Inst. 52 (1970) 34–47.
[30] A.K. Saxena, K.D.P. Nigam, Axial dispersion in laminar flow of polymer solutions through coiled tubes, 26 (1981) 3475–3486.
[31] R.K. Shah, S.D. Joshi, Convective heat transfer in curved ducts, in: S. Kakac, R.K. Shah, Wind Aung (Eds.), Handbook of Single Phase Convective Heat Transfer, Wiley, New York, 1987, pp. 5.1–5.47.
[32] R.K. Shah, M.S. Bhatti, Laminar convective heat transfer in ducts, in: S. Kakac, R.K. Shah, Wind Aung (Eds.), Handbook of Single Phase Convective Heat Transfer, Wiley, New York, 1987, pp. 3.1–3.147.
[33] R.P. Singh, P. Mishra, Frictional factor for Newtonian and non-Newtonian fluid flow in curved pipes, J. Chem. Eng. Jpn. 13 (1980) 275–280.
[34] T. Takami, K. Sudou, Y. Tomita, Flow of non-Newtonian fluid in curved pipes, Bull. JSME 29 (257) (1986a) 3750–3754.
[35] T. Takami, K. Sudou, Y. Tomita, Flow on non-Newtonian fluid in curved pipes, Bull. JSME 29 (257) (1986b) 3755–3760.
[36] J.M. Tarbell, M.R. Samuels, Momentum and heat transfer in helical coils, Chem. Eng. J. 5 (1973) 117–127.
[37] L.H. Thomas, Elliptic Problems in Linear Difference Equations Over A Network, Watson Science Computer Laboratory Department, Columbia University, New York, 1949.
[38] C.M. White, Streamlines flow through curved pipes, Proc. R. Soc. Lond. Ser. A. 123 (1929) 645–663.
[39] P.J. Nandapurkar, M. Raja Rao, Laminar flow heat transfer in power law fluid in helical coils, Indian J. Technology 17 (1979) 308–312.